Plant, Cell and Environment,Volume 43, Issue 1, January 2020, pp. 76-86
DOI:10.1111/pce.13664

Corresponding author details:

Agustin Zsögön

Universidade Federal de Viçosa, Brazil

EM: agustin.zsogon@ufv.br

Title: Control of water-use efficiency by florigen

Authors: Jessenia M. Robledo[1]; David Medeiros[1]; Mateus H. Vicente[2]; Aristéa A. Azevedo[1]; 11 Andrew J. Thompson[3]; Lázaro E. P. Peres[2]; Dimas M. Ribeiro[1]; Wagner L. Araújo[1]; Agustin Zsögö[1]

Affiliations

[1]*Departamento de Biologia Vegetal, Universidade Federal de Viçosa, 36570-900, Viçosa,* 15 *MG, Brazil*

[2]*Laboratory of Hormonal Control of Plant Development. Departamento de Ciências* 17 *Biológicas (LCB), Escola Superior de Agricultura "Luiz de Queiroz", Universidade de São*

Paulo, CP 09, 13418-900, Piracicaba, SP, Brazil

19 [3]*Cranfield Soil and Agrifood Institute, Cranfield University, Cranfield, Bedfordshire, MK43* 20 *0AL, UK*

Author Contributions

JMR and MHV generated the plant material and conducted experiments, JMR, DM and MHV conducted experiments and prepared figures and/or tables. AAA, DMR and WLA designed experiments, contributed reagents/materials/ analysis tools, and reviewed drafts of the article. AJT, LEPP and AZ conceived and designed the experiments, analyzed the data, and wrote the manuscript.

Corresponding author: AZ, agustin.zsogon@ufv.br

Abstract

A major issue in modern agriculture is water loss through stomata during photosynthetic carbon assimilation. In water-limited ecosystems, annual plants have strategies to synchronize their growth and reproduction to the availability of water. Some species or ecotypes flower early to ensure that their life cycles are completed before the onset of late season terminal drought ("drought escape"). This accelerated flowering correlates with low water use efficiency (*WUE*). The molecular players and physiological mechanisms involved in this coordination are not fully understood. We analyzed *WUE* using gravimetry, gas exchange and carbon isotope discrimination in florigen deficient (*sft* mutant), wild-type (Micro-Tom) and florigen over-expressing (*SFT-ox*) tomato lines. Increased florigen expression led to accelerated flowering time and reduced *WUE.* The low *WUE* of *SFT-ox* was driven by higher stomatal conductance and thinner leaf blades. This florigen-driven effect on *WUE* appears be independent of abscisic acid (ABA). Our results open a new avenue to increase *WUE* in crops in an ABA-independent manner. Manipulation of florigen levels could allow us to produce crops with a life cycle synchronized to water availability.

Published by Wiley. This is the Author Accepted Manuscript issued with: Creative Commons Attribution Non-Commercial License (CC:BY:NC 4.0).
The final published version (version of record) is available online at DOI:10.1111/pce.13664. Please refer to any applicable publisher terms of use.

Keywords: abscisic acid, *CENTRORADIALIS/TERMINAL FLOWER 1/SELF PRUNING* (*CETS*) gene family, florigen, flowering, *NOTABILIS*, *SINGLE FLOWER TRUSS*, *Solanum lycopersicum*, water-use efficiency

Introduction

Agriculture is the largest consumer of fresh water in the world. Even though only 18% of the cultivated land is irrigated, the value of its output represents 45% of the total yearly agricultural output. Demand for irrigation water is expected to increase in the coming years in the face of population growth, shifts in diets and climate change, adding strain on the available water supplies (Vörösmarty, Green, Salisbury & Lammers 2000; Damerau, Waha & Herrero 2019). Thus, achieving an efficient use of irrigation water is fundamental for sustainable agricultural production (Fischer, Byerlee & Edmeades 2014). Given the correlation between water use and crop yield, an understanding of the physiological and developmental links between them could assist crop breeding (Sinclair 2018).

Water-use efficiency (*WUE*) is the ratio of plant output to water input (Condon, Richards, Rebetzke & Farquhar 2004). Intrinsic *WUE* (WUE_i) in the leaf is independent of evaporative demand and is the ratio of photosynthetic CO_2 assimilation (A) to stomatal conductance (g_s); it can be improved by either increasing A or decreasing g_s, or both. Generally, reduction in g_s leads to reduction in A, although the relationship is non-linear. $WUE_i = A/g_s$ can be measured instantaneously via gas exchange, or estimated from carbon isotope discrimination ($\Delta^{13}C$) to give a long-term, time-integrated proxy that reflects WUE_i in theory (Farquhar, Ehleringer & Hubick 1989) and also in practice in many species, including tomato (Xu *et al.* 2008). In whole plants, *WUE* can be determined gravimetrically as the ratio of biomass gain to transpiration; at the field scale, yield is related to water inputs as rainfall and irrigation. Genetic improvement of *WUE* requires changes that would either increase yield with similar water use, or lower water use without penalizing yield (Condon *et al.* 2004).

Although transgenic improvement of *WUE* has been achieved by moderately reducing g_s alongside minor depression in A (Thompson *et al.* 2007), conventional breeding for *WUE* has generally not been achieved by direct effects on A or g_s at the leaf level (Richards 2006; Richards, Hunt, Kirkegaard & Passioura 2014). Instead, plant architecture, root development

or time to flowering have been modified to allow water to be captured and used effectively when and where it is available (Franks, Sim & Weis 2007). In collections of Arabidopsis ecotypes, a strong positive correlation was reported between long-term WUE_i and time to flowering (McKay, Richards & Mitchell-Olds 2003; Kenney, McKay, Richards & Juenger 2014) such that early flowering is associated with low WUE_i. The evolved strategy may be to attain the highest rates of CO_2 assimilation in the absence of stomatal limitation to achieve maximum growth prior to an early reproductive transition. In this way, the profligate use of stored soil water (and low *WUE*) allows faster biomass accumulation and greater reproductive fitness, provided that it occurs before soil water becomes limiting. Plant genotypes with conservative strategies in natural ecosystems that leave soil water for future use would be selected against due to competition with rapidly growing profligate neighbors. In contrast, conservative behavior in a crop monoculture would be beneficial if soil water is preserved for later growth; the breeder's challenge is to identify conservative alleles at key loci that might improve *WUE*.

Florigen, encoded by *FLOWERING LOCUS T* (*FT*) in Arabidopsis, acts as a molecular signal to trigger flowering (Turck, Fornara & Coupland 2008; Wigge 2011), and can influence stomatal aperture through blue-light dependent activation of guard cell proton pumps (Kinoshita *et al.* 2011). *FT* is a member of the *CETS* (*CENTRORADIALIS*, *CEN*; *TERMINAL FLOWER 1*, *TFL1*; *SELF-PRUNING*, *SP*) gene family (Wickland & Hanzawa 2015). In tomato, flowering and growth habit are controlled by the *FT* ortholog, *SINGLE FLOWER TRUSS* (*SFT*) (Lifschitz *et al.* 2006), also a key driver of increased yield, whereby *sft* heterozygous plants produce more inflorescences per shoot (Krieger, Lippman & Zamir 2010). The possibility that florigen represents the molecular link between flowering time and *WUE* prompted us to assess *WUE* in tomato genotypes with different levels of *SFT* expression in the genetic background of cv. Micro-Tom (MT). Lines with altered abscisic acid (ABA) levels with known high and low *WUE* were used as controls.

Materials and Methods

Plant material and growth conditions

Tomato (*Solanum lycopersicum* L.) cv. Micro-Tom (MT) plants were used in all experiments. The genotypes are described in detail in Table S1. Briefly, we analysed genotypes with increased and reduced expression of *SFT* and additionally, plants with increased and reduced expression of ABA biosynthesis. MT seeds were provided by Dr. Avram Levy (Weizmann Institute of Science, Israel) in 1998 and subsequently maintained (through self-pollination) as a true-to-type cultivar. The *single flower truss* (*sft*) and *notabilis* (*not*) loss-of-function mutations were introgressed into MT to produce near-isogenic lines using the procedure described by Carvalho *et al.*, (2011). Seeds of *sft* and *not* in their original backgrounds (LA2460, probably cv. Ailsa Craig; and LA0617, cv. Lukullus, respectively) were donated by Dr. Roger Chetelat (Tomato Genetics Resource Center, Davis, California). The *NCED*-ox line in the MT background derives from the sp12 line (originally named d9) in the cv. Ailsa Craig harboring the *NCED* (9-cis-epoxycarotenoid dioxygenase) tomato gene driven by the Gelvin Superpromoter. The transgene was introgressed in MT through crossing as described (Carvalho *et al*., 2011). The *35S::SFT* construct was a kind gift of Prof. Eliezer Lifschitz (Technion-Israel Institute of Technology, Haifa) and used to genetically transform MT as described (Pino *et al.* 2010). Seeds were sown and plants were grown in semi-controlled glasshouse conditions as described previously (Silva *et al.* 2018). Briefly, mean temperature of 28°C, 11.5-h/13-h (winter/summer) photoperiod, 250 to 350 mmol m^2 s^{-1} PAR, and irrigation to field capacity once a day. Seeds were germinated in 350-mL pots with a 1:1 (v/v) mixture of commercial potting mix (Basaplan; Base Agro) supplemented with 1 g L^{-1} 10:10:10 NPK and 4 g L^{-1} dolomite limestone (MgCO3 + CaCO3). Upon appearance of the first true leaf, seedlings of each genotype were transplanted to pots containing the soil mix described above, except for the NPK supplementation, which was increased to 8 g L^{-1}.

Growth analyses

Immediately after anthesis, which occurred at different times for each genotype, we determined branching pattern, length of third, fourth and fifth internodes, number of leaves up to the first inflorescence and on the main shoot (MS) (leaves of primary shoot plus leaves on sympodial units following the first inflorescence) and height of the plant on the primary shoot (MS).

Whole plants were harvested and the dry weight (DW), total leaf area (LA) and specific leaf area (SLA) were evaluated. LA was measured by digital image analysis using a scanner (Hewlett Packard Scanjet G2410, Palo Alto, California, USA) and the images were later processed using the ImageJ® software. SLA was calculated using the following equation:

$$SLA\ (cm^2.\ g^{-1}) = \frac{Leaf\ area}{Leaf\ dry\ weight}$$

Water loss determinations

For water loss measurements, the terminal leaflets of the third leaf were detached from six different 42-day old plants and floated in MES-KCl buffer (5mM KCl, 10 mM MES, 50 µM $CaCl_2$, pH 6.15) with the abaxial side down in Petri dishes and incubated under continuous illumination (120 µE m^{-2} s^{-1}) at 25ºC for 2 h to induce stomatal opening. Water loss was determined gravimetrically over 4 h at the indicated time points. Water loss was then calculated as a percentage of the initial fresh weight.

Carbon isotope composition analysis

The third, fully expanded leaf of five plants per treatment were harvested and ground to fine powder. Samples were sent to the Laboratory of Stable Isotopes (CENA, USP, Piracicaba, Brazil), where they were analysed for $^{13}C/^{12}C$ ratio using a mass spectrometer coupled to a Dumas elemental analyser ANCA-SL (Europa Scientific, Crewe, UK). Carbon isotope ratios were obtained in δ-notation, where

$$\delta = \left(\frac{R}{R_{\text{standard}}}\right) - 1$$

and R and R_{standard} are the isotope ratios of the plant sample and the Vienna Pee Dee Belemnite (VPDB) standard, respectively. $\delta^{13}C$ of atmospheric CO_2 was assumed to be −8 per mil. The $\delta^{13}C$ values for the samples were then converted to carbon isotopic discrimination values, $\Delta^{13}C = (\delta_a - \delta_p)/(1 + \delta_p)$, where δ_a is the $\delta^{13}C$ of atmospheric CO_2 and δ_p the $\delta^{13}C$ of the material(Farquhar *et al.* 1989).

Infrared leaf thermography

For thermal imaging analysis, representative plants were photographed. Thermal images were obtained using an infrared camera (FLIR systems T360, Nashua, USA) and the photos were processed by FLIR Tools + version 5.2 software. The leaf temperature was measured in eight plants of each genotype using an infrared thermometer (LASERGRIP GM400, Guangzhou, China). All measurements were obtained from 42-day old plants at 12:00 in the greenhouse.

Gas exchange and chlorophyll fluorescence measurements

Gas exchange parameters were determined simultaneously along with chlorophyll *a* (Chl *a*) fluorescence measurements using an open-flow infrared gas exchange analyzer system (LI-6400XT; LI-COR Inc., Lincoln, NE) equipped with an integrated fluorescence chamber (LI-6400-40; LI-COR Inc.). Instantaneous gas exchange was measured in the second leaf from top to the base in four 42-day-old plants after 1 h illumination during the light period under photon flux density (1000 μmol m^{-2} s^{-1}). The reference CO_2 concentration was set at 400 μmol CO_2 mol^{-1} air. All measurements were performed at 25 °C, and the leaf-to-air vapor pressure deficit was kept at 1.2-1.8 kPa, while the amount of blue light was set to 10% PPFD to optimize stomatal aperture. Data obtained were analyzed in the Curve Expert (Version 1.4 Image Pro-Plus® software (version 4.5, Media Cybernetics, Silver Spring, USA).

The initial fluorescence (F_0) was measured by illuminating dark-adapted leaves (1 h) with weak modulated measuring beams (0.03 μmol m^{-2} s^{-1}). A saturating white light pulse (8000 μmol m^{-2} s^{-1}) was applied for 0.8 s to obtain the maximum fluorescence (F_m), from which the variable-to-maximum Chl fluorescence ratio, was then calculated: $F_v/F_m = [(F_m - F_0)/F_m)]$. In light-adapted leaves, the steady-state fluorescence yield (F_s) was measured with the application of a saturating white light pulse (8000 μmol m^{-2} s^{-1}) to achieve the light-adapted maximum fluorescence (F_m'). A far-red illumination (2 μmol m^{-2} s^{-1}) was applied after turning off the actinic light to measure the light-adapted initial fluorescence (F_0'). The capture efficiency of excitation energy by open photosystem (PS) II reaction centers (F_v'/F_m') was estimated as described (Logan, Adams & Demmig-Adams 2007) and the actual PSII photochemical efficiency (φ_{PSII}) was estimated as $\varphi_{PSII} = (F_m' - F_s)/F_m'$(Genty, Briantais & Baker 1989).

As φ_{PSII} represents the number of electrons transferred per photon absorbed in the PSII, the electron transport rate (J_{flu}) was calculated as $J_{flu} = \varphi_{PSII}. \alpha. \beta. PPFD$, where α is leaf absorptance and β reflect the partitioning of absorbed quanta between PSII and PSI, and the product $\alpha\beta$, was adopted of the literature to C3 plants (Flexas *et al.* 2007). Dark respiration (R_d) was measured using the same gas exchange system as described above after at least 1 h during the dark period and it was divided by two ($R_d/2$) to estimate the mitochondrial respiration rate in the light (R_L) (Niinemets & Sack 2006).

Determination of mesophyll conductance (g_m), maximum rate of carboxylation (V_{cmax}), maximum rate of carboxylation limited by electron transport (J_{max}) and photosynthetic limitations

The responses of A_N to C_i (A_N/C_i curves) were performed at 1000 μmol m^{-2} s^{-1} at 25 °C under ambient O_2. Briefly, the measurements started at the ambient CO_2 concentration (C_a) of 400 μmol mol^{-1} and once the steady state was reached, C_a was decreased stepwise to 50 μmol mol^{-1}. Upon completion of the measurements at low C_a, C_a was returned to 400 μmol mol^{-1} to restore the original A_N. Next, C_a was increased stepwise to 1600 μmol mol^{-1} for a total of 13 different C_a values (Long & Bernacchi 2003). Corrections for the leakage of CO_2 into and water vapor out of the leaf chamber of the LI-6400 were applied to all gas exchange data as described (Rodeghiero, Niinemets & Cescatti 2007). A_N/C_i curves were obtained using the terminal leaflet of the 2nd fully expanded leaf from the top to the base in four different plants per genotype from 42 days old. The CO_2 concentration in the carboxylation sites (C_c) was calculated according to Harley et al(Harley, Loreto, Di Marco & Sharkey 1992) as:

$$C_c = \Gamma^* [J_{flu}+8 (A_N + R_L)]/ [J_{flu} - 4(A_N + R_L)]$$

where the conservative value Γ* for C3 plants was taken from the same authors. g_m was estimated as described (Ethier & Livingston 2004).

From A_N/C_i and A_N/C_c curves, the maximum carboxylation velocity (V_{cmax}) and the maximum capacity for electron transport rate (J_{max}) were calculated by fitting the mechanistic model of CO_2 assimilation (Farquhar, von Caemmerer & Berry 1980), using the C_i and C_c based on temperature of kinetic parameters of Rubisco (K_c and K_o) (Walker, Ariza, Kaines, Badger &

Cousins 2013). While, V_{cmax}, J_{max} and g_m were normalized to 25ºC using previously described temperature response equations (Sharkey, Bernacchi, Farquhar & Singsaas 2007).

To further investigate the photosynthetic responses we calculated the limitations as described (Grassi & Magnani 2005). Thus, these methods use the values of A_N, g_s, g_m, V_{cmax}, Γ^*, C_c, K_m and $K_m=K_c$ (1+ O/K_o) and permits the partitioning into the functional components of photosynthetic constraints related to stomatal (l_s), mesophyll (l_m), and biochemical (l_b) limitations as shown below:

$$l_s = \frac{(\frac{g_{tot}}{g_s} x \frac{\partial A_N}{\partial C_c})}{(g_{tot} + \frac{\partial A_N}{\partial C_c})}$$

$$l_m = \frac{\left(\frac{g_{tot}}{g_m} x \frac{\partial A_N}{\partial C_c}\right)}{g_{tot} + (\frac{\partial A_N}{\partial C_c})}$$

$$l_b = \frac{g_{tot}}{(g_{tot} + \partial A_N / \partial C_c)}$$

g_{tot} is the total conductance to CO_2 from ambient air to chloroplasts: ($g_{tot} = 1/[(1/g_s)+(1/g_m)]$). The partial derivative $\partial A_N/\partial C_c$ was calculated as:

$$\frac{\partial A_N}{\partial C_c} = ([V_{cmax}(\Gamma^* + K_m)])/(C_c + K_m)$$

Stomatal opening and closure kinetics

Stomatal conductance (g_s) values were recorded at intervals of 30 s using the same gas exchange system described above. The g_s responses to dark/light/dark transitions were measured in the second leaf from top to the base in four 42-day-old plants adapted to the dark for at least two hours. Light in the chamber was kept turned off, and then turned on/turned off for 2/30/30 min. The CO_2 concentration in the chamber was 400 µmol mol^{-1} air. For

responses to CO_2 concentration transitions leaves were exposed to 400/800/400 μmol mol^{-1} CO_2 air for 10/30/30 min under PPFD of 1000 μmol m^{-2} s^{-1}.

Leaf anatomy and histology

Lateral leaflets of the third leaf from five 42-day-old plants were cleared in 95% methanol and transferred to 100% lactic acid, conditioned in a water bath at 95 °C until the leaf presented a completely translucent appearance. Sections were mounted on glass slides, and the samples of adaxial and abaxial epidermis were analyzed with photomicroscope Zeiss AxioScope A1 model (Thornwood, NY, USA) with an attached Axiovision® 105 color image capture system. Images obtained in the photomicroscope were evaluated in the Image Pro-Plus® software (version 4.5, Media Cybernetics, Silver Spring, USA). Stomatal density and stomatal index of the adaxial and abaxial faces (the ratio of stomata to stomata plus other epidermal cells) were determined in at least 6 fields of 0.05 mm^2 per leaf from five different plants as described (Zsögön, Alves Negrini, Peres, Nguyen & Ball 2015).

A fragment of 1 × 0.5 cm of 2nd central leaflet from the top to the base of four different plants from 42 days old was fixed in FAA 70%, and then dehydrated in an ethanol series (70%, 85% and 95%), and infiltrated in historesin (Leica microsystems, Wetzlar, Germany). Cross-sections of 5 μm thickness were stained with 0.05% toluidine blue and analyzed in light microscope (Zeiss AxioScope A1 model Thornwood, NY, USA) with image capture system Axiovision® 105 coupled color. Images were processed in Image Pro-Plus® software (version 4.5, Media Cybernetics, Silver Spring, USA) to quantify abaxial and adaxial epidermal thickness, whole leaf thickness, palisade parenchyma thickness, spongy parenchyma thickness and percentage of intercellular spaces analyzing nine fields per replicate.

Stomatal aperture bioassays

The response of intact leaves to the exogenous application of abscisic acid (ABA) or mannitol was evaluated to assess stomatal function. The third leaf from five 42-day-old plants was detached and floated in MES-KCl buffer medium under light, for 2.5 h to allow stomata to open, then ABA was added to the buffer solution. Leaves with the abaxial side up on open Petri dishes under a direct light source (120 μE m^{-2} s^{-1}) at 25ºC and 70-80% relative humidity

in the plant growth chambers for 2 h. Subsequently control (solvent control), mannitol and ABA were added to the opening buffer to a final concentration of 0.1%, 20 mM and 5 µM, respectively. After 2 h of incubation stomatal aperture was evaluated. Leaf impressions were taken from the abaxial surface of the leaf with dental resin imprints(Berger & Altmann 2000). Nail polish copies were made using a colorless glaze (Von Groll, Berger & Altmann 2002). Samples were analyzed with the aid of a Zeiss AxioScope A1 photomicroscope with an attached Axiovision® 105 color image capture system. Images obtained were evaluated in the Image Pro-Plus® software (version 4.5, Media Cybernetics, Silver Spring, USA). At least 100 stomata per genotype were analyzed.

Gene expression quantification

Quantitative real-time PCR (qRT-PCR) analysis was performed as described (Silva *et al.* 2018) with total RNA isolated from the third terminal leaflet of plants after anthesis in four biological replicates and at least two technical replicates, harvesting and immediately snap-freezing the samples in liquid nitrogen. For RNA extraction, we used TRIzol® (Ambion, Life Technology, Waltham, USA) following the manufacturer's manual. Digestion with DNase I (Ambion; was performed according to the manufacturer's instructions. The integrity of the RNA was checked on 1% (w/v) agarose gels, and the concentration was measured after DNase I digestion using a Multiskan GO^{TM} spectrophotometer (Thermo scientific, Massachusetts, USA) cDNA was synthesized using SuperScript III reverse transcriptase (Invitrogen, Carsbad California) according to the manufacturer's instructions.

For gene expression analyses Power SYBR® green PCR Master Mix was used in MicroAmp^{TM} Optical 96-well reaction plates (both from Applied Biosystems, Singapore) and adhesive film MicroAmp^{TM} Optical (Applied Biosystems, Foster City, CA, USA). The number of reactions from the cycle threshold (CT) as well as the efficiency of the reaction was estimated using the Real-Time PCR Miner tool (Zhao & Fernald 2005). Relative expression was normalized using actin, one constitutively expressed gene; actin was used to calculate ΔΔCT assuming 100% efficiency of amplification of genes ($2^{-\Delta\Delta CT}$). The relative transcript abundance of *SFT* was analyzed to confirm the genotypes. The primer sequences for actin (endogenous) and *SINGLE FLOWER TRUSS* (*SFT*) were *ACTIN* (Solyc03g078400) *Fwd* 5'-GGTCCCTCTATTGTCCACAG-3' and *Rev* 5'-TGCATCTCTGGTCCAGTAGGA-3'; *SFT*

(Solyc03g063100) *Fwd* 5'-GACCCTGATGCTCCAAGTCC-3' and *Rev* 5'-GTGACCAACCAGTGAAGGTATTC-3'.

Experimental design and statistical analysis

The data were obtained from the experiments using a completely randomized design using MT, *sft* and *SFT-ox*. Data are expressed as the mean ± standard error (SE). Data were submitted to one-way analysis of variance (ANOVA), followed by Tukey's honestly significant difference (HSD) test ($P < 0.05$) if the one-way ANOVA result was significant.Real-Time gene expression results were submitted to the Kruskal-Wallis one-way ANOVA test ($P < 0.05$). All the statistical analyses were performed using the Assistat version 7.7 (Campina Grande, Brazil).

Results

SINGLE FLOWER TRUSS negatively influences water-use efficiency in tomato

All genotypes showed the expected phenotype based on previously published work (Fig. 1). *SFT* transcript levels were low for *sft* and high for *SFT-ox* as expected, while *not* and *NCED-ox* were similar to MT, suggesting that ABA levels did not influence expression of *SFT* under these well-watered conditions (Fig. 1). As predicted from the known action of florigen, *SFT-ox* flowered early at 19 days, and *sft* flowered late at 57.3 days, compared to 43.5 days for MT (Table S2). *SFT-ox* plants were considerably smaller since vegetative development largely ceased at the time of flowering in MT, a determinate cultivar harbouring the *self-pruning* (*sp*) mutant allele (Pnueli *et al.* 1998). In our well-watered experiments, although *NCED* overexpression delayed flowering, it did not affect the number of leaves to first flower (Table S2), consistent with its unaltered *SFT* transcript levels (Thompson *et al.* 2007). ABA effects on flowering are known to depend on environment in Arabidopsis: under drought, ABA induced flowering by stimulating *FT* expression (Riboni, Robustelli Test, Galbiati, Tonelli & Conti 2016), but, under well-watered conditions, ABA repressed expression of *SOC1*, a key transcription factor promoting flowering (Riboni *et al.* 2016).

Low *sft* expression led to increased WUE_i (Fig. 1) in the absence of significant differences in mesophyll conductance to CO_2 (g_m) and photosynthetic assimilation rates (A) (Table S3), suggesting that increased WUE_i was the result of reduced g_s. Reduced g_s in turn decreased

leaf water loss, also observed as a higher leaf temperature due to lower evaporative cooling (Fig. S2). The *SFT-ox* line showed decreased *WUE* (determined gravimetrically, Fig. S4) mainly through reduction in dry mass gain (Table S4). $\Delta^{13}C$ was lower in the *sft* mutant (indicating high WUE_i; Fig. 1) and, across all genotype means, $\Delta^{13}C$ had the expected inverse correlation with A/g_s (Fig. 1), confirming that our estimates of WUE_i were consistent whether measured in the short-term or in the long-term. These results were further confirmed when *WUE* was measured gravimetrically in whole plants: *sft* again had 9.7% higher *WUE* and *SFT-ox* had 24.3% lower *WUE* (Fig. S4, Table S4).

SINGLE FLOWER TRUSS induces anatomical modifications in tomato leaves

Higher *SFT* expression had a positive effect on specific leaf area (SLA; Fig. S3), due to decreased leaf thickness (Fig. 2). Leaf thickness tends to be positively correlated with WUE_i because there is more photosynthetic activity per unit area with little impact on g_s (Poorter, Niinemets, Poorter, Wright & Villar 2009).

SFT expression levels did not affect stomatal size or density (Tables S5 and S6), nor the relative velocity of stomatal response to either changes in irradiance or CO_2 concentration, but they did effect steady-state g_s values (Fig. 3). *sft* mutant plants could not reach the same g_s as MT plants under saturating irradiance, whereas *SFT*-ox plants maintained higher g_s values in the dark which would reduce *WUE* by increasing non-productive water loss when no net assimilation was occurring.

SINGLE FLOWER TRUSS controls stomatal conductance (g_s) independently of abscisic acid (ABA) in tomato

Abscisic acid (ABA) is one of the key molecular controllers of stomatal aperture and the signalling pathways are well-characterized (Munemasa *et al.* 2015), so we assessed exogenous application of ABA for interaction with SFT in the control of stomatal aperture. We found an independent and opposite effect of SFT and ABA on stomatal aperture, but not an interaction between them (Fig. 3; Table S7). ABA levels were not significantly altered in *sft* or *SFT*-ox compared to MT (Fig. 3), nor were *SFT* transcript levels altered in *not* or NCED-ox lines with altered ABA levels (Fig. 1).

Discussion

Breeding crops with improved *WUE* is desirable in the face of a growing population with changing dietary profile (Fischer *et al.* 2014). In many species, *WUE* is strongly correlated with flowering time, as selection may have favored synchronization of plant phenology with seasonal moisture (Kenney *et al.* 2014). In Arabidopsis, for instance, pleiotropy of the flowering/vernalization gene *FRIGIDA* in part causes the correlation between phenology and drought physiology (Lovell *et al.* 2013). Tomato does not have a vernalization response, instead, we have shown that SFT, the tomato florigen (Shalit *et al.* 2009), appears to be a key player in the adaptive coordination of *WUE* and flowering time. Identification of florigen as the molecular link between time to flowering and *WUE* provides a new target for improving *WUE* via crop breeding. We have analyzed extremes in florigen expression, but genome engineering or wild relatives could be harnessed to produce alleles with intermediate expression levels or altered patterns of expression (Zsögön, Cermak, Voytas & Peres 2017). SFT had a strong influence on leaf thickness, with concomitant changes in specific leaf area, SLA, which is inversely correlated with *WUE* (Hoffmann, Franco, Moreira & Haridasan 2005). The extension or reduction of the vegetative growth phase in SFT deficient and overproducing lines, respectively, could lead to changes in leaf structure that impact photosynthetic performance, water relations and thus *WUE*. For instance, leaf size tends to be optimized for a given environment (Parkhurst & Loucks 1971), and the positive correlation between increased individual leaf size and *WUE* has adaptive value under limited water availability (Dudley 1996a b).

SFT expression levels do not influence the relative velocity of stomatal response to either changes in irradiance or CO_2 concentration, but rather steady-state g_s values. *sft* mutant plants cannot reach the same g_s as MT plants under saturating irradiance, whereas *SFT*-ox plants maintain higher g_s values in the dark. This suggests that SFT may be a necessary molecular player to relay environmental information allowing fine-tuning of stomatal aperture (Lawson, von Caemmerer & Baroli 2010; Lawson & Blatt 2014). Many mechanisms allow the relay of environmental information for fine-tuning of stomatal aperture (Lawson & Blatt 2014; Matthews, Vialet-Chabrand & Lawson 2018). In a drought escape strategy, SFT may have the role of increasing the setpoint of stomatal aperture under a range of conditions to maximise assimilation rate and thereby allow sufficient biomass to accumulate prior to early flowering. The stomatal effects of SFT and ABA appear to act through independent

pathways, so the molecular intermediates between SFT and activation of the H^+-ATPases that trigger guard cell movements remain to be unveiled (Kim, Böhmer, Hu, Nishimura & Schroeder 2010).

ABA is one of the key molecular controllers of guard cell movement and stomatal aperture (Munemasa *et al.* 2015). ABA can, furthermore, either stimulate or inhibit flowering, depending on environmental conditions, particularly water availability. In Arabidopsis plants undergoing drought conditions ABA will induce flowering by stimulating *FT* expression (Riboni *et al.* 2016). Under well-watered conditions, on the other hand, ABA represses the flowering promoter *SUPPRESSOR OF OVEREXPRESSION OF CONSTANS 1* (*SOC1*), a key transcription factor integrating floral cues in the meristem (Riboni *et al.* 2016). We assessed the potential interaction of ABA with SFT in the control of stomatal aperture. We found an independent and opposite effect of SFT and ABA on stomatal aperture, but not an interaction between them. The stomatal effects of SFT and ABA do not appear to act through the same pathway, so this suggests a potential novel target in breeding for increased *WUE*.

Conclusion

Identification of florigen as a key player linking flowering time and water-use efficiency (*WUE*) paves the way for its exploitation in crop breeding. The universality of the genes of the florigen family makes them a promising target to engineer increased *WUE* in many crops. We explored the changes in florigen dosage in a determinate tomato background harboring a null allele of the anti-florigenic signal SP (Silva *et al.* 2018). The precise molecular mechanism through which florigen controls *WUE* is hitherto unclear, as both direct (*e.g.* stomatal conductance) and indirect (*e.g.* leaf blade thickness) pathways were found to contribute synergistically. Further work should dissect this coordination to unveil the precise molecular pathways involved. Identification of favorable combinations of alleles for ideal florigenic SFT/anti-florigenic SP ratios could lead to plants better adapted to specific agricultural systems in terms of increased yield (Park *et al.* 2014) and *WUE*. Perturbations to these pathways have the potential to uncouple high *WUE* from late flowering; the ability to fine-tune flowering to water availability patterns whilst also achieving higher *WUE* could contribute to sustainable intensification.

Acknowledgements

The Agency for the Support and Evaluation of Graduate Education (CAPES-Brazil), the National Council for Scientific and Technological Development (CNPq-Brazil) and the Foundation for Research Assistance of the São Paulo State (FAPESP-Brazil) provided student scholarships. The Royal Society (NMG\R2\170027), and the Global Challenges Research Fund (UK Research and Innovation) provided grants to AJT and AZ.

Supplemental data

Supplemental Figure 1. *SINGLE FLOWER TRUSS* affects photosynthetic capacity in tomato.

Supplemental Figure 2. Water loss and leaf temperature in tomato genotypes with different florigen expression level.

Supplemental Figure 3. Leaf area and leaf thickness in tomato genotypes with different florigen expression level.

Supplemental Figure 4. Gravimetric water-use efficiency in tomato genotypes with altered expression levels of 9-*cis*-epoxycarotenoid dioxygenase (*NCED*) and *SINGLE FLOWER TRUSS* (*SFT*).

Supplemental Table 1. Description of the genotypes in the Micro-Tom background used in this work.

Supplemental Table 2. Phenological parameters under the control of *SINGLE FLOWER TRUSS* in tomato.

Supplemental Table 3. Photosynthetic characterization of tomato genotypes with different *SINGLE FLOWER TRUSS* expression.

Supplemental Table 4. Gravimetric water-use efficiency in genotypes with different *SINGLE FLOWER TRUSS* expression level in tomato.

Supplemental Table 5. Absence of effect of *SINGLE FLOWER TRUSS* on stomatal size in tomato.

Supplemental Table 6. Absence of effect of *SINGLE FLOWER TRUS*S on stomatal density and stomatal index in tomato.

Supplemental Table 7. *SINGLE FLOWER TRUSS* affects stomatal aperture independently of ABA in tomato.

Literature cited

Berger D. & Altmann T. (2000) A subtilisin-like serine protease involved in the regulation of stomatal density and distribution in *Arabidopsis thaliana*. *Genes & Development*, *14*, 1119–1131.

Carvalho R.F., Campos M.L., Pino L.E., Crestana S.L., Zsögön A., Lima J.E., … Peres L.E. (2011) Convergence of developmental mutants into a single tomato model system: "Micro-Tom" as an effective toolkit for plant development research. *Plant Methods*, *7*, 18.

Condon A.G., Richards R.A., Rebetzke G.J. & Farquhar G.D. (2004) Breeding for high water-use efficiency. *Journal of Experimental Botany*, *55*, 2447–2460.

Damerau K., Waha K. & Herrero M. (2019) The impact of nutrient-rich food choices on agricultural water-use efficiency. *Nature Sustainability*, *2*, 233–241.

Dudley S.A. (1996a) The response to differing selection on plant physiological traits: Evidence for local adaptation. *Evolution*, *50*, 103–110.

Dudley S.A. (1996b) Differing selection on plant physiological traits in response to environmental water availability: A test of adaptive hypothesis. *Evolution*, *50*, 92–102.

Ethier G.J. & Livingston N.J. (2004) On the need to incorporate sensitivity to CO_2 transfer conductance into the Farquhar-von Caemmerer-Berry leaf photosynthesis model. *Plant, Cell and Environment*, *27*, 137–153.

Farquhar G.D., von Caemmerer S. & Berry J.A. (1980) A biochemical model of photosynthetic CO_2 assimilation in leaves of C3 species. *Planta*, *149*, 78–90.

Farquhar G.D., Ehleringer J.R. & Hubick K.T. (1989) Carbon isotope discrimination and photosynthesis. *Annual Review of Plant Physiology and Plant Molecular Biology*, *40*, 503–537.

Fischer A., Byerlee D. & Edmeades G. (2014) *Crop yields and global food security: Will yield increase continue to feed the world?* Australian Centre for International Agricultural Research, Canberra, Australia.

Flexas J., Ortuno M.F., Ribas-Carbo M., Diaz-Espejo A., Florez-Sarasa I.D. & Medrano H. (2007) Mesophyll conductance to CO_2 in *Arabidopsis thaliana*. *New Phytologist*, *175*, 501–511.

Franks S.J., Sim S. & Weis A.E. (2007) Rapid evolution of flowering time by an annual plant in response to a climate fluctuation. *Proceedings of the National Academy of Sciences*, *104*, 1278–1282.

Genty B., Briantais J.M. & Baker N.R. (1989) The relationship between the quantum yield of photosynthetic electron-transport and quenching of chlorophyll fluorescence. *Biochimica et Biophysica Acta*, *990*, 87–92.

Grassi G. & Magnani F. (2005) Stomatal, mesophyll conductance and biochemical limitations to photosynthesis as affected by drought and leaf ontogeny in ash and oak trees. *Plant, Cell and Environment*, *28*, 834–849.

Von Groll U., Berger D. & Altmann T. (2002) The subtilisin-like serine protease SDD1 mediates cell-to-cell signaling during Arabidopsis stomatal development. *Plant Cell*, *14*, 1527–1539.

Harley P.C., Loreto F., Di Marco G. & Sharkey T.D. (1992) Theoretical considerations when estimating the mesophyll conductance to CO_2 flux by analysis of the response of photosynthesis to CO_2. *Plant Physiology*, *98*, 1429–1436.

Hoffmann W.A., Franco A.C., Moreira M.Z. & Haridasan M. (2005) Specific leaf area explains differences in leaf traits between congeneric savanna and forest trees. *Functional Ecology*, *19*, 932–940.

Kenney A.M., McKay J.K., Richards J.H. & Juenger T.E. (2014) Direct and indirect selection

on flowering time, water-use efficiency (WUE, $\delta^{13}C$), and WUE plasticity to drought in Arabidopsis thaliana. *Ecology and Evolution*, *4*, 4505–4521.

Kim T.-H., Böhmer M., Hu H., Nishimura N. & Schroeder J.I. (2010) Guard cell signal transduction network: Advances in understanding abscisic acid, CO_2, and Ca^{2+} signaling. *Annual Review of Plant Biology*, *61*, 561–591.

Kinoshita T., Ono N., Hayashi Y., Morimoto S., Nakamura S., Soda M., … Shimazaki K.I. (2011) FLOWERING LOCUS T regulates stomatal opening. *Current Biology*, *21*, 1232–1238.

Krieger U., Lippman Z.B. & Zamir D. (2010) The flowering gene SINGLE FLOWER TRUSS drives heterosis for yield in tomato. *Nature Genetics*, *42*, 459–463.

Lawson T. & Blatt M.R. (2014) Stomatal size, speed, and responsiveness impact on photosynthesis and water use efficiency. *Plant Physiology*, *164*, 1556–1570.

Lawson T., von Caemmerer S. & Baroli I. (2010) Photosynthesis and stomatal behaviour. *Progress in Botany*, *72*, 265–304.

Lifschitz E., Eviatar T., Rozman A., Shalit A., Goldshmidt A., Amsellem Z., … Eshed Y. (2006) The tomato FT ortholog triggers systemic signals that regulate growth and flowering and substitute for diverse environmental stimuli. *Proceedings of the National Academy of Sciences of the United States of America*, *103*, 6398–6403.

Logan B.A., Adams W.W. & Demmig-Adams B. (2007) Avoiding common pitfalls of chlorophyll fluorescence analysis under field conditions. *Functional Plant Biology*, *34*, 853–859.

Long S.P. & Bernacchi C. (2003) Gas exchange measurements, what can they tell us about the underlying limitations to photosynthesis? Procedures and sources of error. *Journal of Experimental Botany*, *54*, 2393–2401.

Lovell J.T., Juenger T.E., Michaels S.D., Lasky J.R., Platt A., Richards J.H., … McKay J.K. (2013) Pleiotropy of *FRIGIDA* enhances the potential for multivariate adaptation. *Proceedings of the Royal Society B: Biological Sciences*, *280*, 20131043.

Matthews J.S.A., Vialet-Chabrand S. & Lawson T. (2018) Acclimation to fluctuating light impacts the rapidity of response and diurnal rhythm of stomatal conductance. *Plant Physiology*, *176*, 1939–1951.

McKay J.K., Richards J.H. & Mitchell-Olds T. (2003) Genetics of drought adaptation in Arabidopsis thaliana: I. Pleiotropy contributes to genetic correlations among ecological traits. *Molecular Ecology*, *12*, 1137–1151.

Munemasa S., Hauser F., Park J., Waadt R., Brandt B. & Schroeder J.I. (2015) Mechanisms of abscisic acid-mediated control of stomatal aperture. *Current Opinion in Plant Biology*, *28*, 154–162.

Niinemets Ü. & Sack L. (2006) Structural determinants of leaf light-harvesting capacity and photosynthetic potentials. In *Progress in Botany*. (eds K. Esser, U.E. Lüttge, W. Beyshlag & J. Murata), pp. 385–419. Springer Verlag, Berlin.

Park S.J., Jiang K., Tal L., Yichie Y., Gar O., Zamir D., … Lippman Z.B. (2014) Optimization of crop productivity in tomato using induced mutations in the florigen pathway. *Nature Genetics*, *46*, 1337–1342.

Parkhurst D.F. & Loucks L. (1971) Optimal leaf size in relation to environment. *Journal of Ecology*, *13*, 505–537.

Pino L.E., Lombardi-Crestana S., Azevedo M.S., Scotton D.C., Borgo L., Quecini V., … Peres L.E. (2010) The Rg1 allele as a valuable tool for genetic transformation of the tomato "Micro-Tom" model system. *Plant Methods*, *6*, 23.

Pnueli L., Carmel-Goren L., Hareven D., Gutfinger T., Alvarez J., Ganal M., … Lifschitz E. (1998) The SELF-PRUNING gene of tomato regulates vegetative to reproductive switching of sympodial meristems and is the ortholog of CEN and TFL1. *Development*, *125*, 1979–1989.

Poorter H., Niinemets Ü., Poorter L., Wright I.J. & Villar R. (2009) Causes and consequences of variation in leaf mass per area (LMA): A meta-analysis. *New Phytologist*, *182*, 565–588.

Riboni M., Robustelli Test A., Galbiati M., Tonelli C. & Conti L. (2016) ABA-dependent

control of *GIGANTEA* signalling enables drought escape via up-regulation of *FLOWERING LOCUS T* in *Arabidopsis thaliana*. *Journal of Experimental Botany*, *67*, 6309–6322.

Richards R.A. (2006) Physiological traits used in the breeding of new cultivars for water-scarce environments. *Agricultural Water Management*, *80*, 197–211.

Richards R.A., Hunt J.R., Kirkegaard J.A. & Passioura J.B. (2014) Yield improvement and adaptation of wheat to water-limited environments in Australia—a case study. *Crop and Pasture Science*, *65*, 676.

Rodeghiero M., Niinemets Ü. & Cescatti A. (2007) Major diffusion leaks of clamp-on leaf cuvettes still unaccounted: How erroneous are the estimates of Farquhar et al. model parameters? *Plant, Cell and Environment*, *30*, 1006–1022.

Shalit A., Rozman A., Goldshmidt A., Alvarez J.P., Bowman J.L., Eshed Y. & Lifschitz E. (2009) The flowering hormone florigen functions as a general systemic regulator of growth and termination. *Proceedings of the National Academy of Sciences of the United States of America*, *106*, 8392–8397.

Sharkey T.D., Bernacchi C.J., Farquhar G.D. & Singsaas E.L. (2007) Fitting photosynthetic carbon dioxide response curves for C3 leaves. *Plant, Cell and Environment*, *30*, 1035–1040.

Silva W.B., Vicente M.H., Robledo J.M., Reartes D.S., Ferrari R.C., Bianchetti R.E., … Zsögön A. (2018) SELF-PRUNING Acts synergistically with DIAGEOTROPICA to guide auxin responses and proper growth form. *Plant Physiology*, *176*, 2904-2016

Sinclair T.R. (2018) Effective water use required for improving crop growth rather than transpiration efficiency. *Frontiers in Plant Science*, *9*, 1442.

Thompson A.J., Andrews J., Mulholland B.J., McKee J.M.T., Hilton H.W., Horridge J.S., … Taylor I.B. (2007) Overproduction of abscisic acid in tomato increases transpiration efficiency and root hydraulic conductivity and influences leaf expansion. *Plant Physiology*, *143*, 1905–1917.

Turck F., Fornara F. & Coupland G. (2008) Regulation and identity of florigen:

FLOWERING LOCUS T moves center stage. *Annual review of plant biology*, *59*, 573–94.

Vörösmarty C.J., Green P., Salisbury J. & Lammers R.B. (2000) Global water resources: vulnerability from climate change and population growth. Science, *289*, 284–288.

Walker B., Ariza L.S., Kaines S., Badger M. & Cousins A.B. (2013) Temperature response of in vivo Rubisco kinetics and mesophyll conductance in *Arabidopsis thaliana*: Comparisons to *Nicotiana tabacum*. *Plant, Cell and Environment*, *36*, 2108–2119.

Wickland D.P. & Hanzawa Y. (2015) The FLOWERING LOCUS T/TERMINAL FLOWER 1 gene family: functional evolution and molecular mechanisms. *Molecular Plant*, *8*, 983–997.

Wigge P. a. (2011) FT, A mobile developmental signal in plants. *Current Biology*, *21*, R374–R378.

Xu X., Martin B., Comstock J.P., Vision T.J., Tauer C.G., Zhao B., … Knapp S. (2008) Fine mapping a QTL for carbon isotope composition in tomato. *Theoretical and Applied Genetics*, *117*, 221–233.

Zhao S. & Fernald R.D. (2005) Comprehensive algorithm for quantitative Real-Time Polymerase Chain Reaction. *Journal of Computational Biology*, *12*, 1047–1064.

Zsögön A., Alves Negrini A.C., Peres L.E.P., Nguyen H.T. & Ball M.C. (2015) A mutation that eliminates bundle sheath extensions reduces leaf hydraulic conductance, stomatal conductance and assimilation rates in tomato (*Solanum lycopersicum*). *New Phytologist*, *205*, 618–626.

Zsögön A., Cermak T., Voytas D. & Peres L.E.P. (2017) Genome editing as a tool to achieve the crop ideotype and de novo domestication of wild relatives: Case study in tomato. *Plant Science*, *256*, 120–130.

Figure Legends

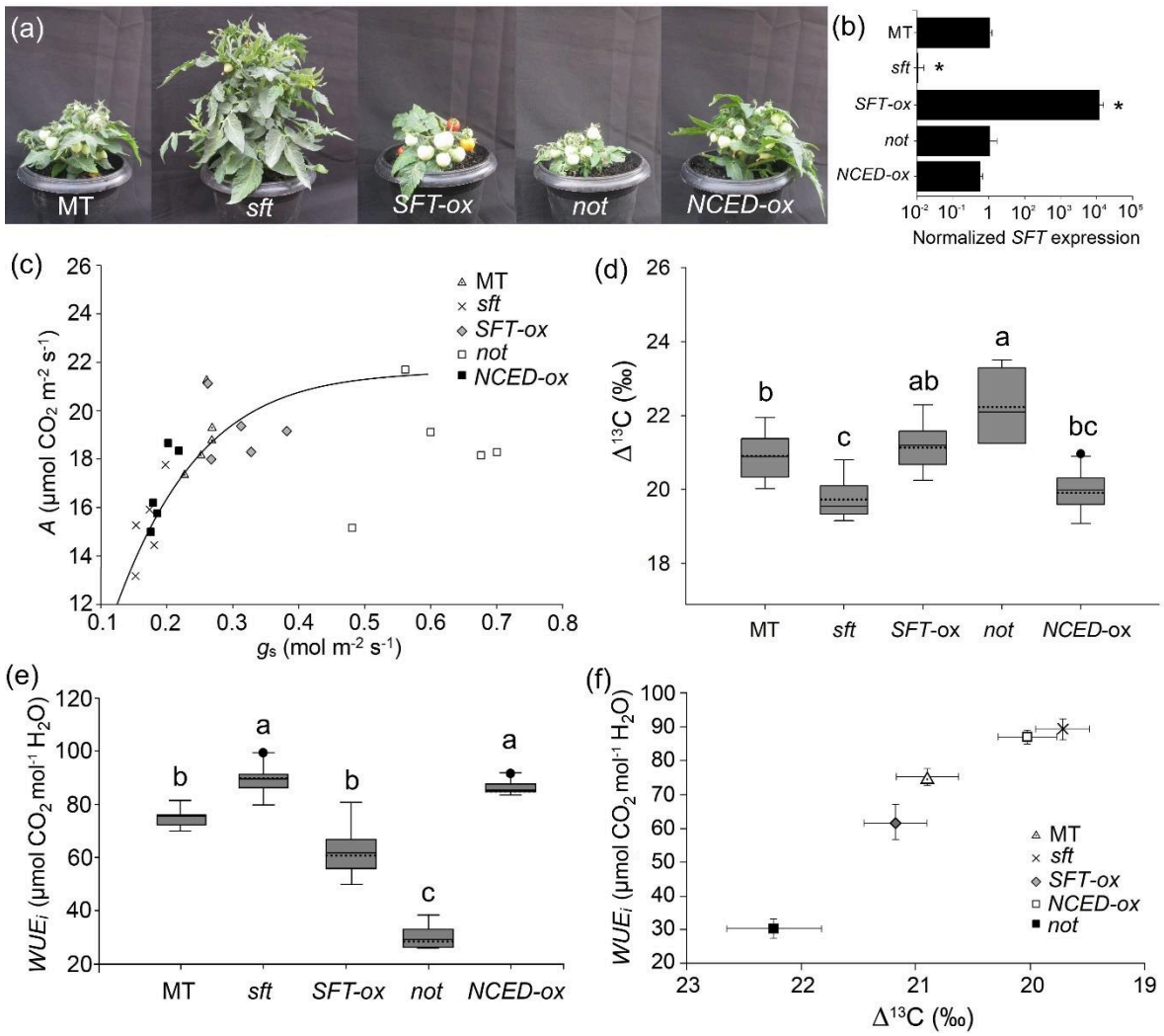

Figure 1. *SINGLE FLOWER TRUSS* influences water-use efficiency in tomato. (a) Representative plants of tomato cv. Micro-Tom (MT), loss-of-function *single flower truss* (*sft*) mutant, transgenic *SFT* over-expression line (*SFT-ox*), abscisic acid deficient loss-of-function 9-*cis*-epoxycarotenoid dioxygenase (*NCED*) mutant *notabilis* (*not*) and *NCED* over-expression line (*NCED-ox*), 75 days after germination. (b) Relative transcript accumulation of *SFT* determined on 42-day-old leaves. Significant differences tested with Kruskal-Wallis test on $2^{-\Delta\Delta Ct}$ values; *p*-value: *0.05. Data was log-transformed and is depicted as means ± s.e.m. (n=4 plants). (c) Relationship between net photosynthesis (A) and stomatal conductance (g_s) determined under saturing light in fully expanded leaves. The solid line indicates a hyperbolic function was fitted to the data. Each point represents measurements on one individual plant. (d) Carbon isotope discrimination ($\Delta^{13}C$) measured in the same leaves as gas exchange, sampled 42 dag. Data are means ± s.e.m (n=6). (e) Intrinsic water-use efficiency (A/g_s) calculated using data shown in panel c. Values are mean ± s.e.m (n=5). (f) Relationship between A/g_s and carbon isotope composition, calculated from data shown in panels d and e. Boxes in box-plots represent IQR, center line the median, dotted line the mean, and the ends of the whisker are set at 1.5*IQR above the third quartile and 1.5*IQR below the first quartile. If the minimum or maximum value falls outside this range, it is considered an outlier and depicted as a full circle. Significant differences tested with one-way ANOVA followed by Tukey's honestly significant difference (HSD) test; letters indicate significant differences, *p*-value < 0.05.

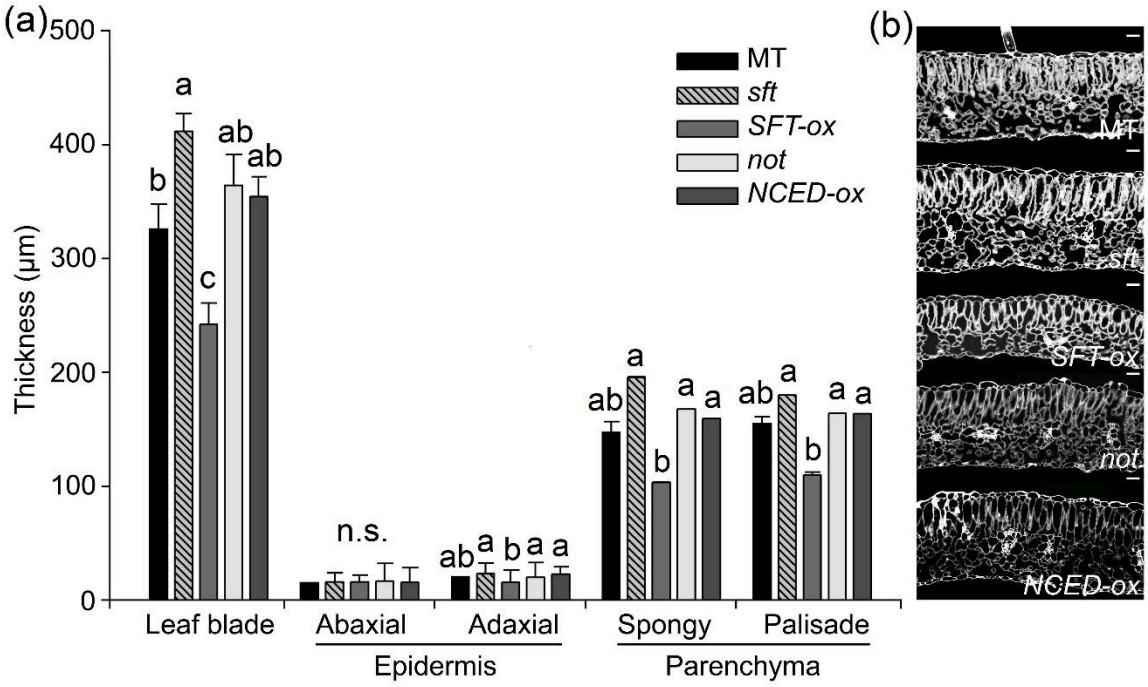

Figure 2. ***SINGLE FLOWER TRUSS*** **induces anatomical modifications in tomato leaves**. (a) Leaf anatomical parameters. Data are means ± s.e.m. (n=4). (b) Representative cross-sectional images of fully expanded terminal leaflets obtained from the second leaf from top in 42-day old plants of tomato cv. Micro-Tom (MT); loss-of-function *single flower truss* (*sft*) mutant; transgenic *SFT* over-expression line (*SFT-ox*); abscisic acid deficient loss-of-function 9-*cis*-epoxycarotenoid dioxygenase (*NCED*) mutant *notabilis* (*not*) and *NCED* over-expression line (*NCED-ox*). Scale bars, 50 µm. Significant differences tested with one-way ANOVA followed by Tukey's honestly significant difference (HSD) test; letters indicate significant differences, p-value < 0.05. (n.s. = non-significant).

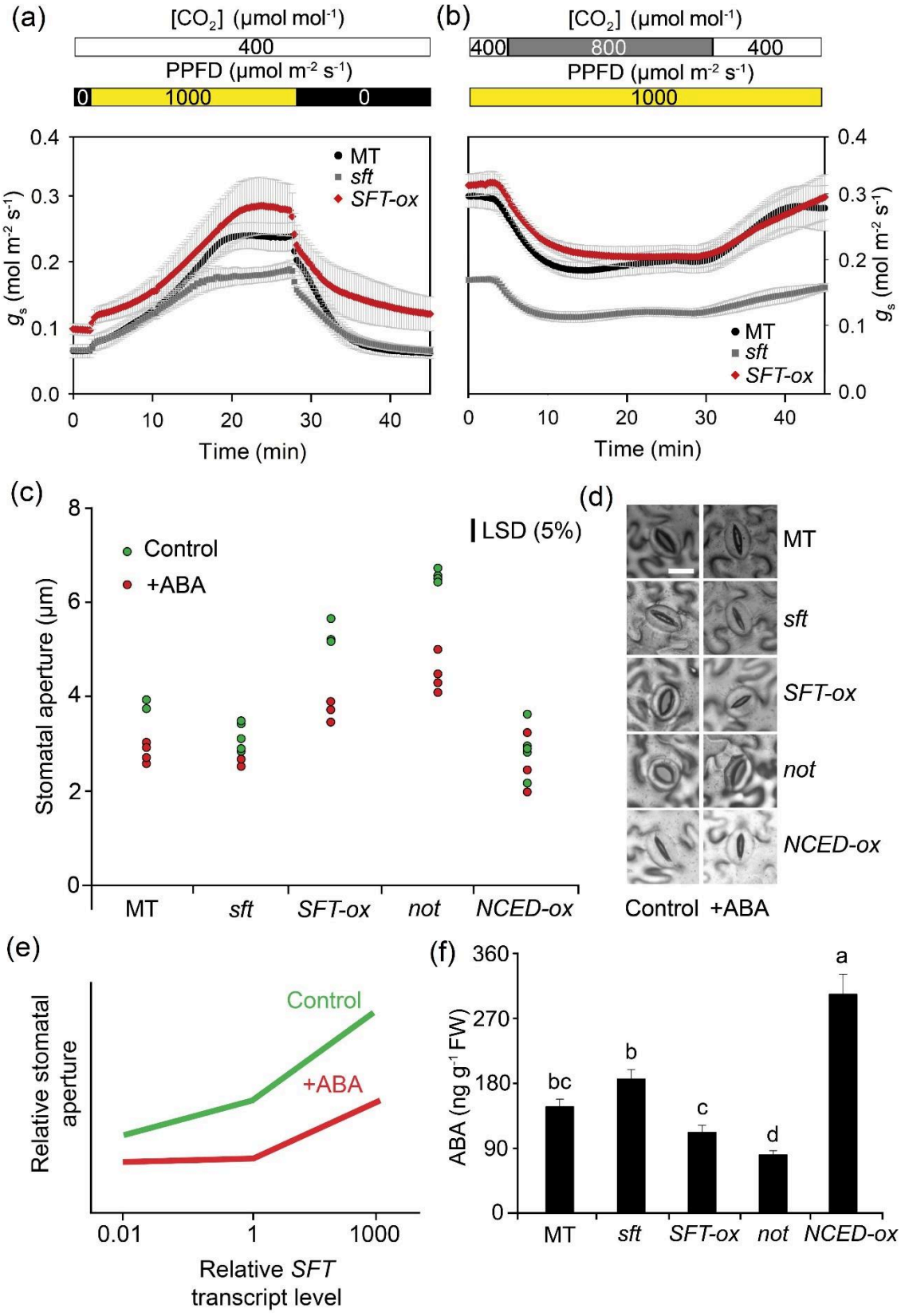
(a)
[CO2] (µmol mol-1)
400
PPFD (µmol m-2 s-1)
0
1000
0
MT
sft
SFT-ox
gs (mol m-2 s-1)
Time (min)
(b)
[CO2] (µmol mol-1)
400
800
400
PPFD (µmol m-2 s-1)
1000
MT
sft
SFT-ox
gs (mol m-2 s-1)
Time (min)
(c)
Control
+ABA
LSD (5%)
Stomatal aperture (µm)
MT
sft
SFT-ox
not
NCED-ox
(d)
MT
sft
SFT-ox
not
NCED-ox
Control
+ABA
(e)
Control
+ABA
Relative stomatal aperture
Relative SFT transcript level
(f)
ABA (ng g-1 FW)
bc
b
c
d
a
MT
sft
SFT-ox
not
NCED-ox

Figure 3. *SINGLE FLOWER TRUSS* controls stomatal conductance (g_s) independently of abscisic acid (ABA) in tomato. Comparison of tomato cv. Micro-Tom (MT) response to changes in (a), photosynthetic photon flux density (PPFD) with loss-of-function *single flower truss* (*sft*) mutant, and transgenic *SFT* over-expression line (*SFT-ox*) and (b), CO_2 concentration. Measurements were performed over three days on attached terminal leaflets of the second leaf fully expanded leaf in 42/45-day-old plants. Data are means ± s.e.m. (n=4). (c) Measurements of stomatal pore width in MT, *sft*, *SFT-ox*, abscisic acid deficient loss-of-function 9-*cis*-epoxycarotenoid dioxygenase (*NCED*) mutant *notabilis* (*not*) and *NCED* over-expression line (*NCED-ox*). Measurements conducted after treatment with control buffer solution or 5 µM ABA solution from the third fully expanded leaf of 42-day-old plants. Each data point is the mean value (n=25 stomata) of one leaf replicate. (d) Representative stomata from light microscopy images in opening buffer (control) or 5 µM ABA. bar=20 µm. (e) Schematic representation of the relationship between *SFT* transcript level and ABA on the control of stomatal aperture. (f) ABA concentration in leaves of the genotypes 42 dag. Data are means ± s.e.m (n=6). Letters indicate significant differences determined by one-way ANOVA followed by Tukey's HSD test, *p*-value < 0.05.

Supplemental data

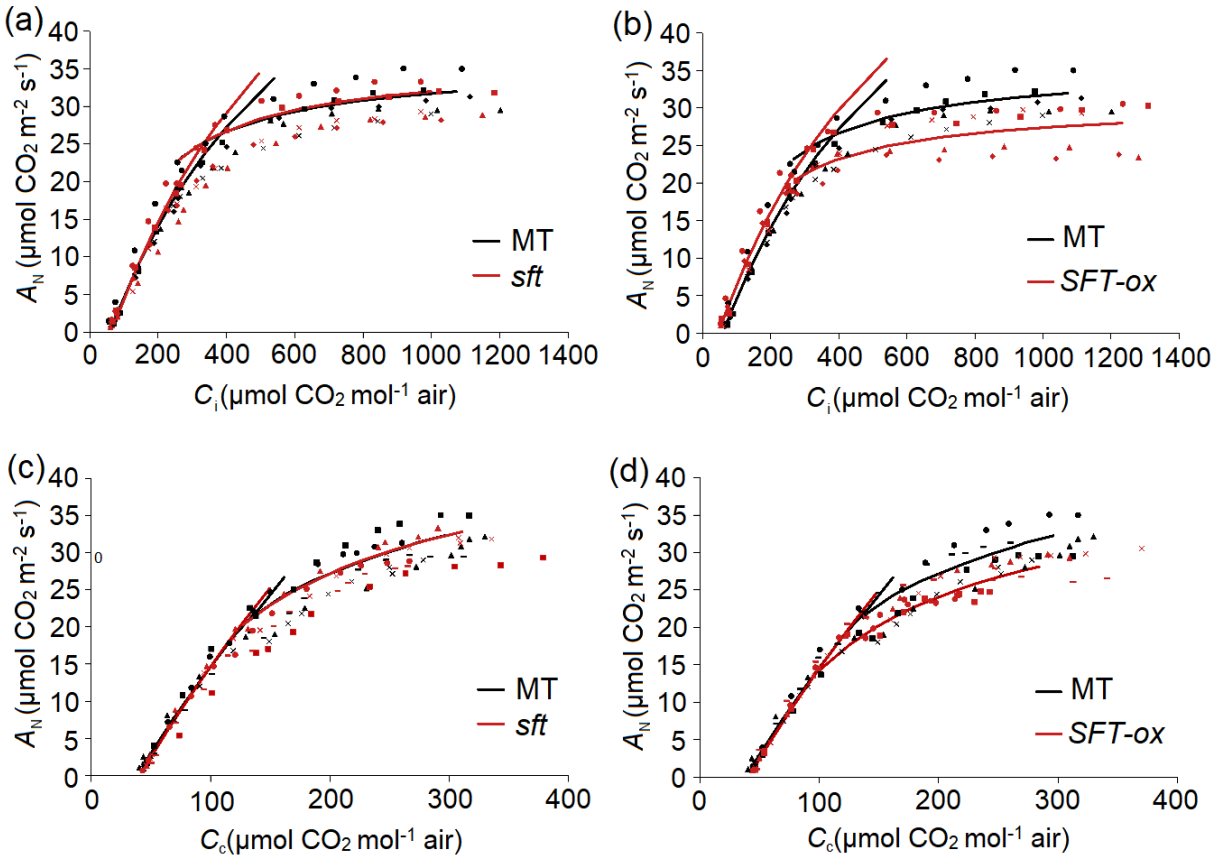

Figure S1. *SINGLE FLOWER TRUSS* affects photosynthetic capacity in tomato. Net photosynthesis (A_N) curves in response to sub-stomatal (C_i) and chloroplastic (C_c) CO_2 concentration in tomato cv. Micro-Tom (MT), loss-of-function *single flower truss* (*sft*) mutant and transgenic *SFT* over-expression line (*SFT-ox*) under saturating light (1000 µmol m^{-2} s^{-1}). Values were obtained using the second fully expanded leaf counting from the apex. The solid line was fitted based on leaf biochemistry parameters.The biochemically based leaf photosynthesis model(Farquhar, von Caemmerer & Berry 1980) was fitted to the data based on C_i or C_c values

of A_N/C_i or A_N/C_c for five plants of MT (black symbols) and *sft* or *SFT-ox* (red symbols). Different symbols were used for each individual plant.

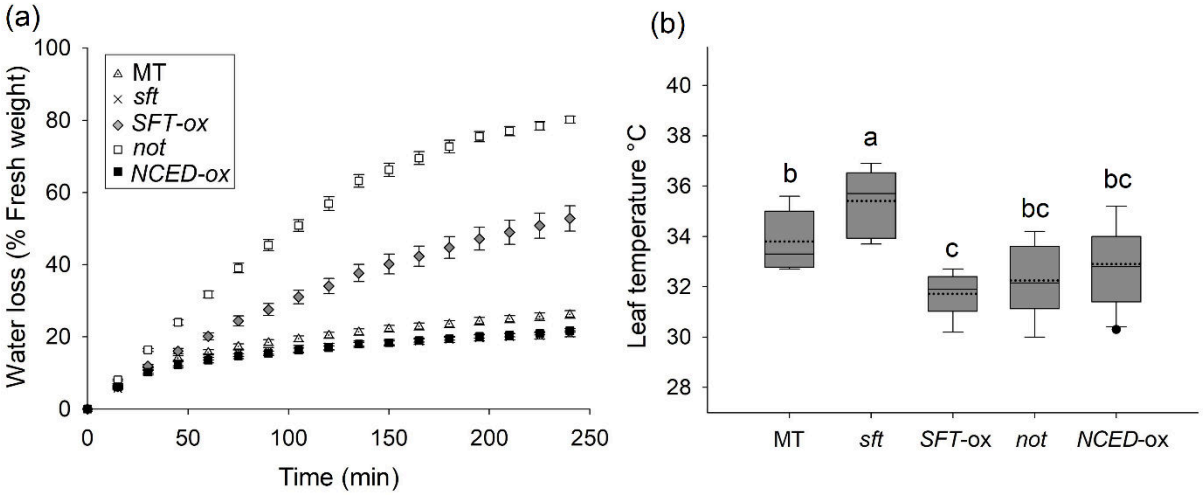

Figure S2. ***SINGLE FLOWER TRUSS*** **influences water loss and leaf temperature in tomato**. (a) Water loss rate in detached terminal leaflet of fully expanded leaves of tomato cv. Micro-Tom (MT), loss-of-function *single flower truss* (*sft*) mutant, transgenic *SFT* over-expression line (*SFT-ox*), abscisic acid deficient loss-of-function 9-*cis*-epoxycarotenoid dioxygenase (*NCED*) mutant *notabilis* (*not*) and *NCED* over-expression line (*NCED-ox*). Values are mean ± s.e.m. (n=6). (b) Leaf surface temperature determined by infrared thermography on the third fully expanded leaf 42 days after germination. Values are mean ± s.e.m. (n=10). Significant differences tested with one-way ANOVA followed by Tukey's honestly significant difference (HSD) test, *p*-value < 0.01

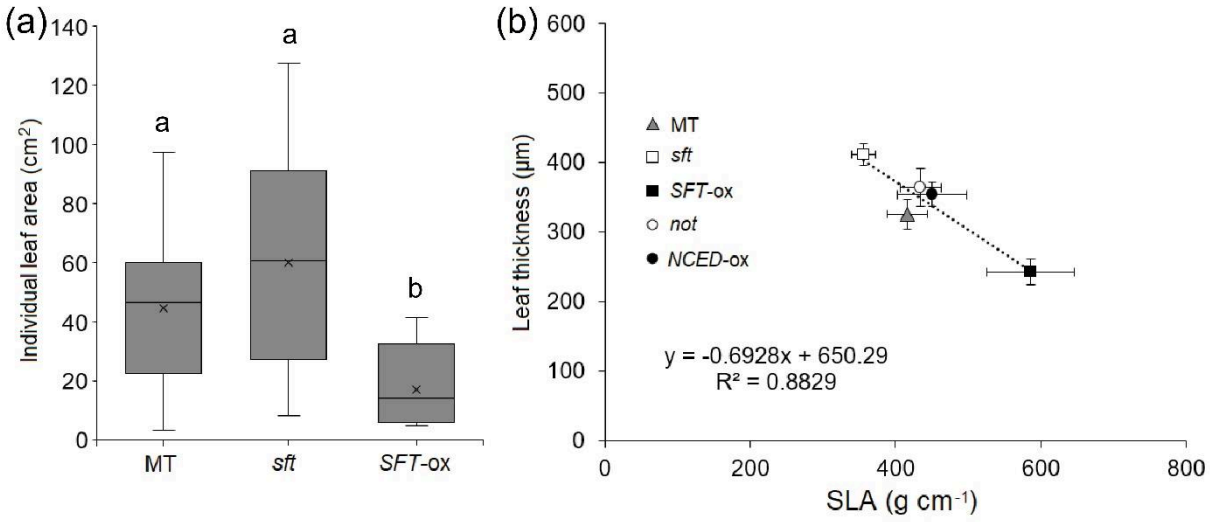

Figure S3. *SINGLE FLOWER TRUSS* alters leaf area and leaf thickness in tomato. (a) Individual leaf area in tomato cv. Micro-Tom (MT), loss-of-function *single flower truss* (*sft*) mutant and transgenic *SFT* over-expression line (*SFT-ox*). Boxes in box-plots represent IQR, center line the median, "x" the mean, and the ends of the whisker are set at 1.5*IQR above the third quartile and 1.5*IQR below the first quartile. If the minimum or maximum value falls outside this range, it is considered an outlier and depicted as a full circle. Significant differences tested with one-way ANOVA followed by Tukey's honestly significant difference (HSD) test, *p*-value < 0.01. Letters indicate significant differences (b) Relationship between leaf lamina thickness and specific leaf area (SLA). Data points are means (n=6) ± s.e.m.

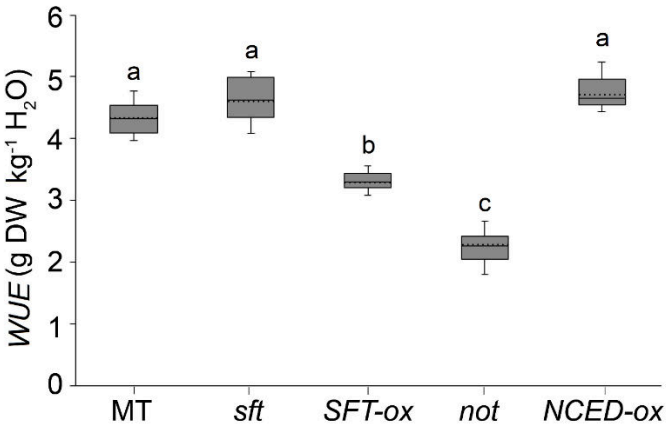

Figure S4. Gravimetric water-use efficiency (*WUE*) is controlled by *SINGLE FLOWER TRUSS* in tomato. Comparison of *WUE* in tomato cv. Micro-Tom (MT), loss-of-function *single flower truss* (*sft*) mutant, transgenic *SFT* over-expression line (*SFT-ox*), abscisic acid deficient loss-of-function 9-*cis*-epoxycarotenoid dioxygenase (*NCED*) mutant *notabilis* (*not*) and *NCED* over-expression line (*NCED-ox*). Boxes in box-plots represent interquartile range (IQR), center line the median, dotted line the mean, and the ends of the whisker are set at 1.5*IQR above the third quartile and 1.5*IQR below the first quartile. Significant differences tested with one-way ANOVA followed by Tukey's honestly significant difference (HSD) test; letters indicate significant differences, *p*-value < 0.01

Table S1. Description of the genotypes in the Micro-Tom background used in this work.

Genotype	Description	References
Micro-Tom (MT)	Harbors the recessive allele *self-pruning* (*sp*), which leads to a determinate growth and uniform fruit ripening; the recessive allele *dwarf* (*d*), which leads to reduced brassinosteroid biosynthesis.	Meissner et al., 1997; Bishop et al., 1999; Martí et al., 2006
single flower truss (*sft*)	*SFT* (Solyc03g063100) codes for the floral inducer 'florigen'. *sft* is a loss-of-function mutation introgressed into MT from its original background (LA2460, possibly cv. Ailsa Craig).	Kerr EA, 1982; Molinero-Rosales et al., 2004; Lifschitz and Eshed, 2006
SFT-ox	Plants with overexpression of *SFT* under the control of cauliflower mosaic virus (CaMV) 35S promoter have a high flowering induction.	Lifschitz et al., 2006
notabilis (not) (LA4487)	*NOT* (Solyc07g056570) codes for A 9-cis-epoxycarotenoid dioxygenase (*NCED*), a key enzyme for oxidative cleavage of 9-cis-epoxycarotenoids in ABA biosynthesis. The *not* mutation was introgressed into MT from its original background (LA0617, cv. Lukullus)	Tal, 1966; Carvalho et al., 2011; Thompson et al., 2004
NCED-ox	Plants overexpressing the *NCED* carotenoid cleavage enzyme under control of a superpromoter (sp) derived from CaMV 35S. The sp12 line, which has an increased ABA level but without increased seed dormancy and guttation, was originally produced in the Ailsa Craig background from which the transgene was introgressed into MT.	Thompson et al., 2000; 2007

Table S2. Phenological parameters under the control of *SINGLE FLOWER TRUSS* in tomato. Comparison of tomato cv. Micro-Tom (MT), loss-of-function *single flower truss* (*sft*) mutant, transgenic *SFT* over-expression line (*SFT-ox*), abscisic acid deficient loss-of-function 9-*cis*-epoxycarotenoid dioxygenase (NCED) mutant *notabilis* (*not*) and *NCED* over-expression line (*NCED-ox*). Data are means ± s.e.m. (n=5). Significant differences tested with one-way ANOVA followed by Tukey's honestly significant difference (HSD) test; letters indicate significant differences p-value < 0.01. For leaves to first flower, significant differences were tested with Kruskal-Wallis p-value < 0.01.

	MT	***sft***	***SFT-ox***	***not***	***NCED-ox***
Days to anthesis	43.5 ± 1.8b	57.3 ± 0.7a	19.0 ± 0.8d	41.5 ± 1.1c	50.2 ± 1.4b
Leaves to 1st flower	6.1 ± 0.31b	12.1 ± 0.17a	2.8 ± 0.4c	5.5 ± 0.2b	5.5 ± 0.2b
Height to 1st flower (cm)	6.1 ± 0.23b	15.0 ± 0.21a	2.7 ± 0.21c	6.1 ± 0.1b	6.3 ± 0.1b
Stem diameter (cm)	5.3 ± 0.24a	5.3 ± 0.09a	3.8 ± 0.1b	5.1 ± 0.1a	5.2 ± 0.1a
2nd internode length (cm)	0.80 ± 0.05b	1.10 ± 0.04a	0.77 ± 0.02b	0.90 ± 0.01b	0.90 ± 0.01b
Specific leaf area ($cm^2\ g^{-1}$)	416.6 ± 28.7b	356.0 ± 16.2b	586.6 ± 59.8a	434.5 ± 28.7ab	450.8 ± 47.8ab

Table S3. Photosynthetic characterization of tomato genotypes with different *SINGLE FLOWER TRUSS* expression. Gas exchange data for tomato cv. Micro-Tom (MT), loss-of-function *single flower truss* (*sft*) mutant, transgenic *SFT* over-expression line (*SFT-ox*), abscisic acid deficient loss-of-function 9-*cis*-epoxycarotenoid dioxygenase (NCED) mutant *notabilis* (*not*) and *NCED* over-expression line (*NCED-ox*). Data are means ± s.e.m. (n=5). Significant differences tested with one-way ANOVA followed by Tukey's honestly significant difference (HSD) test; letters indicate significant differences p-value < 0.05.

Parameters*	**MT**	***sft***	***SFT-ox***
C_i **(µmol CO_2 mol^{-1})**	255.59 ± 6.74	248.41 ± 6.31	260.12 ± 4.43
C_c **(µmol CO_2 mol^{-1})**	132.9 ± 2.39a	119.67 ± 4.66b	137.64 ± 3.57a
g_m **(mol CO_2 m^{-2} s^{-1} bar^{-1})**	0.16 ± 0.01	0.19 ± 0.03	0.17 ± 0.01
$V_{cmax}\_C_i$ **(µmol m^{-2} s^{-1})**	82.63 ± 3.61	93.15 ± 9.32	86.01 ± 2.38
$V_{cmax}\_C_c$ **(µmol m^{-2} s^{-1})**	165.76 ± 5.34	176.24 ± 4.46	173.63 ± 2.02
$J_{max}\_C_i$ **(µmol m^{-2} s^{-1})**	153.46 ± 6.68a	166.96 ± 14.37a	130.05 ± 5.76b
$J_{max}\_C_c$ **(µmol m^{-2} s^{-1})**	184.04 ± 5.07a	194.11 ± 6.88a	170.28 ± 2.15b
$J_{max}\_C_i$ **:** $V_{cmax}\_C_i$	1.86 ± 0.04a	1.82 ± 0.08a	1.51 ± 0.06b
$J_{max}\_C_c$ **:** $V_{cmax}\_C_c$	1.11 ± 0.01a	1.1 ± 0.02a	0.98 ± 0.02b
Stomatal limitation	0.37 ± 0.02	0.43 ± 0.02	0.37 ± 0.01
Mesophyll limitation	0.36 ± 0.01	0.31 ± 0.03	0.35 ± 0.02
Biochemical limitation	0.28 ± 0.02	0.26 ± 0.02	0.29 ± 0.01

* C_i, sub-stomatal CO_2 concentration; C_c, Chloroplastic CO_2 concentration; g_m, mesophyll condutance to CO_2 estimated according to Harley et al.(Harley, Loreto, Di Marco & Sharkey 1992); $V_{cmax}\_C_i$ or $\_C_c$, maximum carboxylation capacity based or C_i or C_c; $J_{max}\_C_i$ or $\_C_c$, maximum capacity for electron transport rate based on C_i or C_c.

Table S4. Gravimetric water-use efficiency (*WUE*) is controlled by *SINGLE FLOWER TRUSS* in tomato. Comparison of tomato cv. Micro-Tom (MT), loss-of-function *single flower truss* (*sft*) mutant, transgenic *SFT* over-expression line (*SFT-ox*), abscisic acid deficient loss-of-function 9-*cis*-epoxycarotenoid dioxygenase (*NCED*) mutant *notabilis* (*not*) and *NCED* over-expression line (*NCED-ox*). Plants were grown in pots containing a closed water reservoir connected to the soil by a wick system. Pots were weighed and lost water replaced daily to the same initial volume over a period of 35 days. Data are means ± s.e.m. (n = 5). Significant differences tested with one-way ANOVA followed by Tukey's honestly significant difference (HSD) test; letters indicate significant differences p-value < 0.01.

	MT	***sft***	***SFT-ox***	***not***	***NCED-ox***
Water transpired (g)	250.0 ± 14.9a	281.0 ± 13.4a	202.0 ± 8.7b	180.0 ± 11.4b	313.0 ± 20.3a
Dry weight gained (g)	1.07 ± 0.06b	1.33 ± 0.13a	0.66 ± 0.04c	0.40 ± 0.03c	1.49 ± 0.12a
WUE (g DW kg^{-1} H_2O)	4.31 ± 0.11a	4.73 ± 0.15a	3.26 ± 0.06b	2.24 ± 0.14c	4.76 ± 0.14a

Table S5. *SINGLE FLOWER TRUSS* does not affect stomatal size in tomato. Guard cells length and width measured in epidermal imprints of tomato cv. Micro-Tom (MT), loss-of-function *single flower truss* (*sft*) mutant and transgenic *SFT* over-expression line (*SFT-ox*). Measurements obtained from the third fully expanded leaf

of 42-days old plants. Data are means ± s.e.m. (n=100 stomata). No significant differences were found using one-way ANOVA.

Parameters	**MT**	***sft***	***SFT-ox***
Length (µm)	32.7 ± 1.1	33.6 ± 1.1	33.8 ± 0.8
Width (µm)	25.3 ± 0.4	23.8 ± 0.3	23.1 ± 0.9
Length x width (μm^2)	835.4 ± 38.1	803.5 ± 34.2	787.8 ± 50.5

Table S6. *SINGLE FLOWER TRUSS* does not affect stomatal density or stomatal index in tomato. Leaf epidermal features in tomato cv. Micro-Tom (MT), loss-of-function *single flower truss* (*sft*) mutant, transgenic *SFT* over-expression line (*SFT-ox*), abscisic acid deficient loss-of-function 9-*cis*-epoxycarotenoid dioxygenase (*NCED*) mutant *notabilis* (*not*) and *NCED* over-expression line (*NCED-ox*). Measurements obtained from the third fully expanded leaf of 42-days old plants. Data are means ± s.e.m. (n=5).

Parameters*		**MT**	***sft***	***SFT-ox***	***not***	***NCED-ox***
SD (mm^{-2})	Adaxial	44.7 ± 2.7b	48.6 ± 10.7b	51.5 ± 11.9b	84.8 ± 14.6a	55.3 ± 12.3b
	Abaxial	95.7 ± 7.5b	99.7 ± 6.1b	109.8 ± 6.9b	132.6 ± 12.0a	100.8 ± 7.7b
PCD (mm^{-2})	Adaxial	290.9 ± 13.2b	293.5 ± 18.8b	293.2 ± 26.7b	332.6 ± 27.3a	301.5 ± 19.3b
	Abaxial	284.8 ± 9.5b	333.4 ± 22.1a	301.5 ± 5.6ab	329.5 ± 20.8a	307.6 ± 18.0ab
SI (%)	Adaxial	13.4 ± 1.5b	14.2 ± 2.8b	15.3 ± 3.8ab	20.2 ± 3.1a	15.2 ± 2.9ab
	Abaxial	24.9 ± 1.7	23.2 ± 1.2	26.7 ± 1.1	28.6 ± 1.1	24.7 ± 1.3

* SD, stomatal density; PCD, pavement cell density; SI, stomatal index.

Table S7. *SINGLE FLOWER TRUSS* affects stomatal aperture independently of ABA in tomato. Results of 2×3 two-way ANOVA using three levels of *SFT* transcript [(as quantified in tomato cv. Micro-Tom (MT), loss-of-function *single flower truss* (*sft*) mutant and transgenic *SFT* over-expression line (*SFT-ox*)] and two levels of ABA (either 0 or 5 µM ABA) as the independent variables. SS, sum of squares; df, degrees of freedom; MS, mean square; HSD (honestly significant difference) is the absolute (unassigned) difference between any two means required for significance at the designated level: HSD[.05] for the .05 level; HSD[.01] for the .01 level. Raw data are plotted in Figure 3a of the main manuscript.

Source	**SS**	**df**	**MS**	**F**	**Critical values**	
					HSD [.05]	**HSD [.01]**
SFT level	185357533.62	1	185357533.62	296.24	120.23	158.33
ABA	275227399.93	2	137613699.97	219.94	176.59	219.68
SFT level × ABA	27570527.63	2	13785263.82	22.03	305.16	359.42
Error	413585693.43	661	625696.96			
Total	871397631.42	666				

References

Bishop G.J., Nomura T., Yokota T., Harrison K., Noguchi T., Fujioka S., … Kamiya Y. (1999) The tomato DWARF enzyme catalyses C-6 oxidation in brassinosteroid biosynthesis. *Proceedings of the National Academy of Sciences of the United States of America*, *96*, 1761–1766.

Carvalho R.F., Campos M.L., Pino L.E., Crestana S.L., Zsögön A., Lima J.E., … Peres L.E. (2011) Convergence of developmental mutants into a single tomato model system: "Micro-Tom" as an effective toolkit for plant development research. *Plant Methods*, *7*, 18.

Farquhar G.D., von Caemmerer S. & Berry J.A. (1980) A biochemical model of photosynthetic CO2 assimilation in leaves of C3 species. *Planta*, *149*, 78–90.

Harley P.C., Loreto F., Di Marco G. & Sharkey T.D. (1992) Theoretical considerations when estimating the mesophyll conductance to CO_2 flux by analysis of the response of photosynthesis to CO_2. *Plant Physiology*, *98*, 1429–1436.

Kerr EA (1982) Single flower truss '"sft"' appears to be on chromosome 3. *Tomato Genetics Cooperative Reports*, *32*, 31.

Lifschitz E. & Eshed Y. (2006) Universal florigenic signals triggered by FT homologues regulate growth and flowering cycles in perennial day-neutral tomato. *Journal of Experimental Botany*, *57*, 3405–3414.

Lifschitz E., Eviatar T., Rozman A., Shalit A., Goldshmidt A., Amsellem Z., … Eshed Y. (2006) The tomato FT ortholog triggers systemic signals that regulate growth and flowering and substitute for diverse environmental stimuli. *Proceedings of the National Academy of Sciences of the United States of America*, *103*, 6398–6403.

Marti E., Gisbert C., Bishop G.J., Dixon M.S. & Garcia-Martinez J.L. (2006) Genetic and physiological characterization of tomato cv. Micro-Tom. *Journal of Experimental Botany, 57*, 2037–2047.

Meissner R., Jacobson Y., Melamed S., Levyatuv S., Shalev G., Ashri A., … Levy A. (1997) A new model system for tomato genetics. *Plant Journal*, *12*, 1465–1472.

Molinero-Rosales N., Latorre A., Jamilena M. & Lozano R. (2004) SINGLE FLOWER TRUSS regulates the transition and maintenance of flowering in tomato. *Planta*, *218*, 427–434.

Tal M. (1966) Abnormal stomatal behavior in wilty mutants of tomato. *Plant Physiology*, *41*, 1387–1391.

Thompson A.J., Jackson A.C., Symonds R.C., Mulholland B.J. & Dadswell A.R. (2000) Ectopic expression of a tomato 9-cis-epoxycarotenoid dioxygenase gene causes over-

production of abscisic acid. *Plant Journal*, *23*, 363–374.

Thompson A.J., Thorne E.T., Burbidge A., Jackson A.C., Sharp R.E. & Taylor I.B. (2004) Complementation of notabilis, an abscisic acid-deficient mutant of tomato: importance of sequence context and utility of partial complementation. *Plant, Cell and Environment*, *27*, 459–471.

Cranfield University

CERES Research Repository **https://dspace.lib.cranfield.ac.uk/**

School of Water, Energy and Environment (SWEE) Staff publications (SWEE)

Control of water-use efficiency by florigen

Robledo, Jessenia M.

2019-11-05

Attribution-NonCommercial 4.0 International

Robledo JM, Medeiros D, Vicente MH. (2020) Control of water-use efficiency by florigen. Plant, Cell and Environment, Volume 43, Issue 1, January 2020, pp. 76-86
https://doi.org/10.1111/pce.13664

Downloaded from CERES Research Repository, Cranfield University